2009

Complex electronic states in double-layered ruthenates (Sr1−xCax)3Ru2O7

Zhe Qu

Jin Peng

David Fobes

Leonard Spinu
University of New Orleans

Zhiqiang Mao

Complex electronic states in double-layered ruthenates $(Sr_{1-x}Ca_x)_3Ru_2O_7$

Zhe Qu,[1] Jin Peng,[1] Tijiang Liu,[1] David Fobes,[1] Leonard Spinu,[2] and Zhiqiang Mao[1,*]

[1]*Department of Physics and Engineering Physics, Tulane University, New Orleans, Louisiana 70118, USA*

[2]*Advanced Material Research Institute and Physics Department, University of New Orleans, New Orleans, Louisiana 70148, USA*

(Received 16 January 2009; revised manuscript received 20 July 2009; published 30 September 2009)

The magnetic ground state of $(Sr_{1-x}Ca_x)_3Ru_2O_7$ $(0 \leq x \leq 1)$ is complex, ranging from an itinerant metamagnetic state $(0 \leq x < 0.08)$ to an unusual heavy-mass nearly ferromagnetic (FM) state $(0.08 < x < 0.4)$, and finally to an antiferromagnetic (AFM) state $(0.4 \leq x \leq 1)$. In this report we elucidate the electronic properties for these magnetic states, and show that the electronic and magnetic properties are strongly coupled in this system. The electronic ground state evolves from an AFM quasi-two-dimensional metal for $x = 1.0$ to an Anderson localized state for $0.4 \leq x < 1.0$ (the AFM region). When the magnetic state undergoes a transition from the AFM to the nearly FM state, the electronic ground state switches to a weakly localized state induced by magnetic scattering for $0.25 \leq x < 0.4$, and then to a magnetic metallic state with the in-plane resistivity $\rho_{ab} \propto T^\alpha$ $(\alpha > 2)$ for $0.08 < x < 0.25$. The system eventually transforms into a Fermi-liquid ground state when the magnetic ground state enters the itinerant metamagnetic state for $x < 0.08$. When x approaches the critical composition $(x \sim 0.08)$, the Fermi-liquid temperature is suppressed to zero Kelvin, and non-Fermi-liquid behavior is observed. These results demonstrate the strong interplay between the charge and spin degrees of freedom in the double-layered ruthenates.

I. INTRODUCTION

The Ruddlesden-Popper series of perovskite ruthenates $(Sr,Ca)_{n+1}Ru_nO_{3n+1}$ have attracted significant attention since they exhibit a wide range of unique electronic and magnetic states. The richness of states in ruthenates is epitomized by unconventional spin-triplet superconductivity,[1–3] antiferromagnetic (AFM) Mott insulating behavior,[4–6] an electronic nematic phase,[7] itinerant magnetism,[8,9] and orbital ordered states.[10–12] These states all occur in close proximity and provide a rare opportunity to tune the system between various states using nonthermal control parameters such as chemical composition, pressure, and magnetic field. Tuning of nonthermal parameters often results in interesting exotic properties.

The double-layered ruthenates $(Sr_{1-x}Ca_x)_3Ru_2O_7$ provide a typical example. The properties of the end members in this series are dramatically different. The $x = 0$ member, $Sr_3Ru_2O_7$, is an enhanced paramagnet showing an itinerant metamagnetic transition.[13] Its electronic properties under magnetic fields remarkably depend on field orientation.[7,14,15] Magnetic field applied along the c axis induces an electronic nematic phase near a metamagnetic quantum critical end point.[7,14,15] In contrast, $Ca_3Ru_2O_7$ $(x = 1)$ is AFM with Néel temperature $T_N = 56$ K (Refs. 16 and 17) and exhibits giant magnetoresistance attributed to a bulk spin-valve effect.[18–21] Recent studies on floating-zone-grown high-quality single crystals of $(Sr_{1-x}Ca_x)_3Ru_2O_7$ revealed rich exotic magnetic properties.[22,23] With Ca substitution for Sr, the system evolves from an itinerant metamagnetic state $(0 \leq x < 0.08)$ to an unusual heavy-mass nearly ferromagnetic (FM) state with an extremely large Wilson ratio $R_w (0.08 < x < 0.4)$. R_w is ~ 10 for $Sr_3Ru_2O_7$ (Ref. 13); it increases to a maximum of ~ 700 near $x = 0.2$.[22] The nearly FM state does not develop a long-range FM order despite considerably strong FM correlations manifested by the large Wilson ratio, but instead

freezes in a cluster-spin-glass (CSG) phase at low temperatures.[22,23] The system eventually switches to a long-range AFM state for $0.4 \leq x \leq 1$,[22,23] in which the magnetic easy axis changes continuously from the c axis to the ab plane with increasing Ca content.[23]

To better understand these complex magnetic phase transitions, information on the electronic states involved in these transitions is needed. The end members of $(Sr_{1-x}Ca_x)_3Ru_2O_7$ have been shown to exhibit distinctly different electronic states; while $Sr_3Ru_2O_7$ exhibits Fermi-liquid behavior,[13] $Ca_3Ru_2O_7$ undergoes a metal-insulator transition (MIT) at 48 K,[16,17] which has been suggested to be caused by the opening of a pseudogap associated with a density wave instability,[24,25] and enters a quasi-two-dimensional (2D) metallic ground state at low temperatures.[17] It is particularly interesting to investigate the evolution of the electronic states between these two end members and how the states are coupled to the magnetic states.

Here, we report a systematic study on the electronic states of the $(Sr_{1-x}Ca_x)_3Ru_2O_7$ solid solution by means of transport and specific heat measurements. We find that the electronic states are complex and strongly coupled with the magnetic states in this system. In the AFM state with $0.4 \leq x < 1.0$, the electronic ground state of the system behaves as an Anderson localized state. In the nearly FM region, however, the system shows different electronic properties: a weakly localized state induced by magnetic scattering is observed for $0.25 \leq x < 0.4$ and a magnetic metallic state with the resistivity $\rho \propto T^\alpha$ $(\alpha > 2)$ occurs for $0.08 < x < 0.25$. When the nearly FM state transforms to a metamagnetic state for $x < 0.08$, the electronic state changes to a Fermi-liquid ground state. The Fermi-liquid temperature is suppressed to zero Kelvin when x approaches the critical value 0.08. Non-Fermi-liquid behavior is also observed in thermodynamic properties near this critical composition.

II. EXPERIMENT

We have succeeded in growing high-quality single-crystal samples of $(Sr_{1-x}Ca_x)_3Ru_2O_7$ in the whole range of x using the floating-zone technique.[22] All crystals selected for measurements were characterized carefully by x-ray diffraction and superconducting quantum interference device (SQUID) magnetometer. Since SQUID has an extremely high sensitivity to ferromagnetic materials, it guarantees that the selected samples do not contain any FM impurity phases such as $(Sr,Ca)_4Ru_3O_{10}$ (Ref. 26) and $(Sr,Ca)RuO_3$.[9] SQUID was also used for magnetization measurements on selected samples. Specific heat measurements were performed using a thermal relaxation method in a Quantum Design PPMS. The electrical transport measurements were carried out in a He^3 cryostat with a base temperature of 0.3 K, using a standard four-probe technique. The crystallographic axes of the samples selected for transport measurements were identified using x-ray Laue diffraction. The electrical current was applied along in-plane Ru-O-Ru bond direction for in-plane resistivity ρ_{ab} measurements and along the c axis for out-of-plane resistivity ρ_c measurements.

III. RESULTS

Figure 1 shows the temperature dependence of resistivity, $\rho_{ab}(T)$ and $\rho_c(T)$, for typical compositions of the $(Sr_{1-x}Ca_x)_3Ru_2O_7$ solid solution series. Like other layered ruthenates with cylindrical Fermi surfaces (FSs),[27–32] $(Sr_{1-x}Ca_x)_3Ru_2O_7$ displays remarkable anisotropy between ρ_{ab} and ρ_c. ρ_c is much higher than ρ_{ab} throughout the entire series. For $Ca_3Ru_2O_7(x=1.0)$, both ρ_{ab} and ρ_c exhibit anomalies at temperatures corresponding to T_N and T_{MIT}; they show metallic behavior immediately below $T_N=56$ K, but a discontinuous increase at $T_{MIT}=48$ K. Below T_{MIT}, ρ_{ab} first increases with decreasing temperature, then exhibits metallic behavior once again at low temperatures. These characteristics are consistent with previous results obtained using floating-zone-grown crystals.[17] Recent studies demonstrate that the low temperature metallic behavior originates from small FS pockets which survive below T_{MIT}.[24] With Sr substitution for Ca, T_N and T_{MIT}, as determined from ρ_{ab}, systematically shift to lower temperatures for $0.4 \leq x < 1$ and are consistent with those obtained early from magnetization measurements.[22] The system still remains an AFM metallic state between T_N and T_{MIT} in this composition range. However in contrast to the first-order-like MIT observed in $Ca_3Ru_2O_7$, the MIT in doped samples occurs in a continuous fashion. Below T_{MIT}, both ρ_{ab} and ρ_c exhibit nonmetallic behavior down to 2K ($d\rho/dT<0$), consistent with the results reported by Iwata *et al.*[23] We also note that ρ_c show anomalies at T_N and T_{MIT} for $0.6<x\leq1$, but only at T_{MIT} for $0.4 \leq x \leq 0.6$. These results suggest that partial Sr substitution for Ca ($0.4 \leq x < 1$) leads the electronic ground state to transform from a quasi-2D metallic state in $Ca_3Ru_2O_7$ to a nonmetallic state. This nonmetallic state can be ascribed to Anderson localization as discussed below.

When $x<0.4$, a magnetic phase transition from the AFM to the heavy-mass nearly FM state occurs.[22,23] This transition is also probed in magnetoresistance measurements, as shown
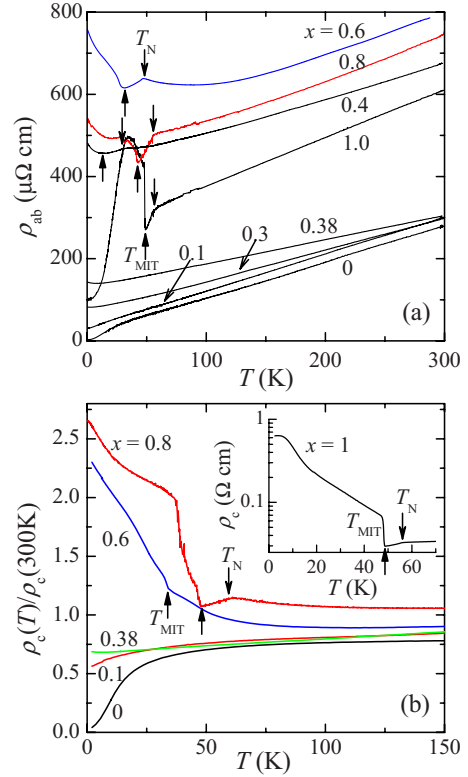

FIG. 1. (Color online) (a) Temperature dependence of in-plane resistivity $\rho_{ab}(T)$ for double-layered ruthenates $(Sr_{1-x}Ca_x)_3Ru_2O_7$. The downward arrow denotes the Néel temperature T_N and the upward arrow marks the metal-insulator transition temperature T_{MIT}. (b) Temperature dependence of out-of-plane resistivity $\rho_c(T)$ (normalized to its 300 K value) for typical compositions. Inset shows ρ_c as a function of temperature for $Ca_3Ru_2O_7$ ($x=1$).

in Fig. 2. For $x \geq 0.4$, a metamagnetic transition with clear hysteresis occurs, ascribed to the spin flip/flop transition of the AFM state. The metamagnetic transition field increases with increasing x and exceeds 6 T for $x \geq 0.8$. In these measurements the magnetic field is applied along the in-plane Ru-O-Ru direction, i.e., the (110) direction in the $Bb2_1m$ space group, which is not the easy axis of
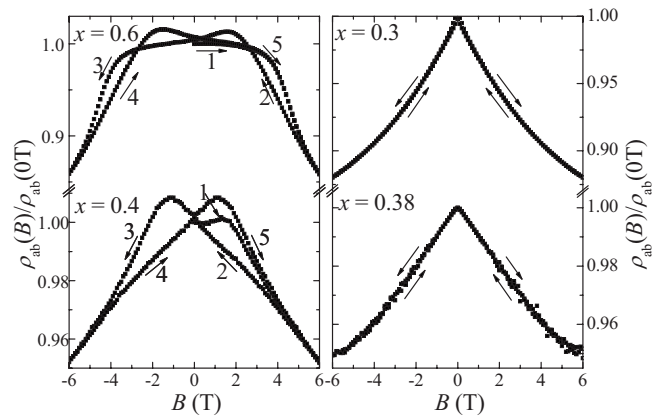

FIG. 2. In-plane resistivity (normalized to its 0 T values) at 0.3 K versus field for $(Sr_{1-x}Ca_x)_3Ru_2O_7$. The magnetic field is applied parallel to the electrical current.
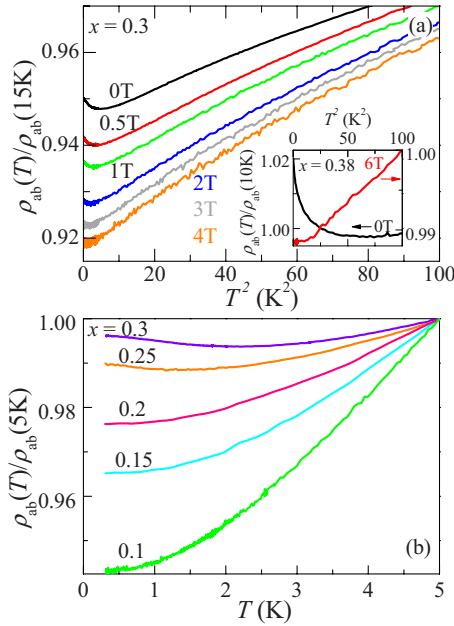
FIG. 3. (Color online) (a) In-plane resistivity (normalized to its 15 K value) plotted versus T^2 under a range of applied fields, for the $x=0.3$ sample. Inset: In-plane resistivity (normalized to its 10 K value) plotted versus T^2 under zero field and 6 T for the $x=0.38$ sample. (b) Temperature dependence of the in-plane resistivity for several samples with $0.1 \leq x \leq 0.3$, normalized to their values at 5 K.

magnetization.[17,33,34] For $x=0.3$ and 0.38, however, a negative magnetoresistance without hysteresis is observed, consistent with the expected result for the nearly FM state.[22,23] Accompanied with the magnetic phase transition, the electronic state changes drastically. As seen in Fig. 1, the resistivity of the nearly FM state in $0.08 < x < 0.4$ is much smaller than that of the AFM state in $0.4 \leq x < 1$. Its temperature dependence shows two different behaviors: for $0.25 \leq x < 0.4$, ρ_{ab} exhibits a small upturn at low temperature [see Fig. 3(b)], suggesting a weakly localized state, while for $0.08 < x < 0.25$, ρ_{ab} shows metallic behavior in the whole temperature range and can be fitted to $\rho \propto T^\alpha (\alpha > 2)$ at low temperatures (e.g., $\alpha=2.7$ for $x=0.2$ [see Fig. 4(a)]). Interestingly, both behaviors are sensitive to magnetic field; a moderate magnetic field can tune them to quasi-quadratic temperature dependences, as shown in Figs. 3(a) and 4(b), suggesting that they are of magnetic origin, which will be discussed below. In contrast, the nonmetallic state in the AFM region with $0.4 \leq x < 1$ is more robust, less sensitive to magnetic field as shown in Fig. 5.

When the Ca content is decreased below $x=0.08$, the system transforms into a metamagnetic Fermi-liquid ground state. As shown in the upper panel of the Fig. 6, the metamagnetic transition can be identified in both resistivity and magnetization for this composition range. In contrast to the spin flip/flop induced metamagnetic transition seen in the samples with $x \geq 0.4$, the metamagnetic transition observed here is reversible between upward and downward field sweeps and this transition is generally interpreted as a field-induced Stoner transition.[14] The metamagnetic transition field B_{IM} depends sensitively on the Ca content; for $x=0$,

$B_{IM} \sim 5.1$ T, consistent with the previous result;[14] B_{IM} decreases rapidly as x increases, down to zero as x approaches the critical value 0.08 (see the inset to the lower panel of Fig. 6). Occurring along with the metamagnetism, as shown in Fig. 7, the resistivity exhibits a quadratic temperature dependence below a characteristic temperature T_{FL}, indicating a Fermi-liquid ground state. The Fermi-liquid temperature T_{FL} is ~ 10 K for $x=0$; it decreases rapidly to ~ 1.95 K for $x=0.02$, and is eventually suppressed to zero near $x=0.08$.

From the above results for various composition ranges, we have constructed an electronic phase diagram for $(Sr_{1-x}Ca_x)_3Ru_2O_7$, and plotted it together with the magnetic phase diagram we obtained earlier,[22] as shown in the upper panel of Fig. 8. To summarize, $Ca_3Ru_2O_7$ shows an AFM metallic state below $T_N=56$ K and then experiences a metal-insulator transition at $T_{MIT}=48$ K, eventually evolving into a quasi-two-dimensional metallic ground state at low temperatures. With Sr substitution for Ca, the metallic state remains
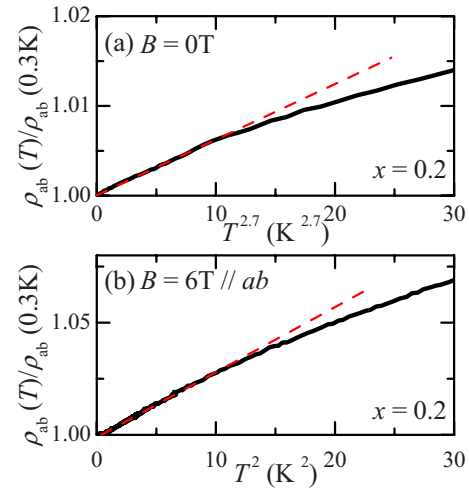

FIG. 4. (Color online) (a) In-plane resistivity (normalized to its value at 0.3 K) plotted versus $T^{2.7}$ under zero field for the $x=0.2$ sample. (b) In-plane resistivity (normalized to its value at 0.3 K) plotted versus T^2 under 6 T for the $x=0.2$ sample.
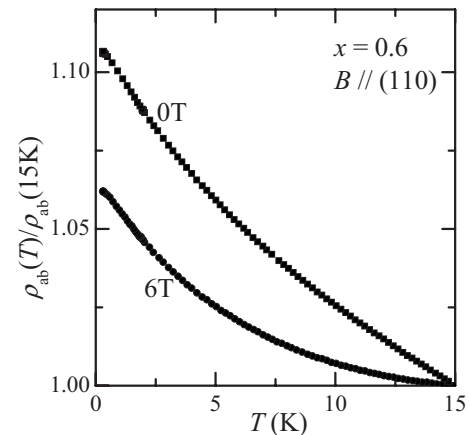

FIG. 5. Temperature dependence of the in-plane resistivity (normalized to its 15 K value) under zero field and 6 T for the $x=0.6$ sample. The magnetic field is applied parallel to the electrical current.
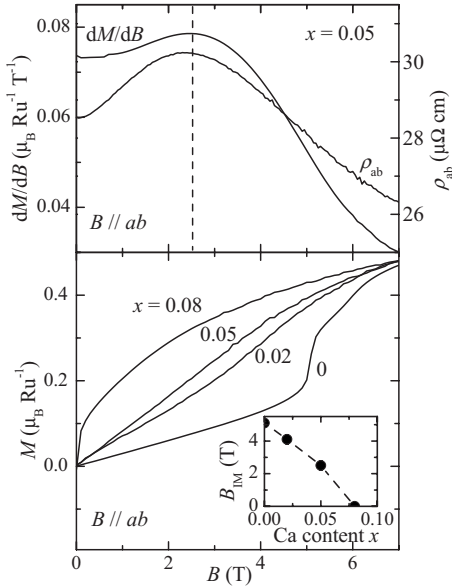
FIG. 6. Upper panel: in-plane resistivity and the first derivative of the magnetization dM/dB as a function of magnetic field at $T = 2$ K for the $x = 0.05$ sample. The dash line marks the metamagnetic transition field B_{IM}. Lower panel: magnetization as a function of magnetic field at 2 K for the samples with $x = 0.08$, 0.05, 0.02, and 0. Inset: the evolution of the metamagnetic transition field as a function of the Ca content.

between T_N and T_{MIT} ($0.4 \leq x < 1$, Region I) and yields to an Anderson localized state caused by disorders as the temperature is decreased below T_{MIT} ($0.4 \leq x < 1$, Region II). When $x < 0.4$, the magnetic ground state switches from the AFM to the nearly FM state that freezes to a CSG phase at low temperatures.[22,23] Accompanying this magnetic phase transition is an electronic ground-state transition from the Anderson localized state to a weakly localized state induced by magnetic scattering ($0.25 \leq x < 0.4$, Region III). Further decrease in x leads to the presence of a magnetic metallic state ($0.08 < x < 0.25$, Region IV). When $x < 0.08$, the system en-
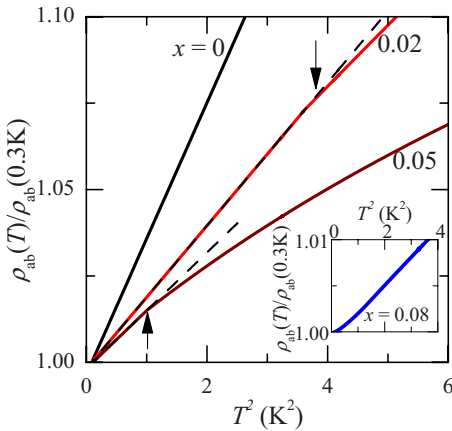

FIG. 7. (Color online) In-plane resistivity (normalized to its 0.3 K value) plotted versus T^2 for several samples with various Ca contents. Arrows indicate the temperature where the curve deviates from linearity, i.e., the Fermi-liquid temperature T_{FL}. Inset shows the data for the $x = 0.08$ sample.
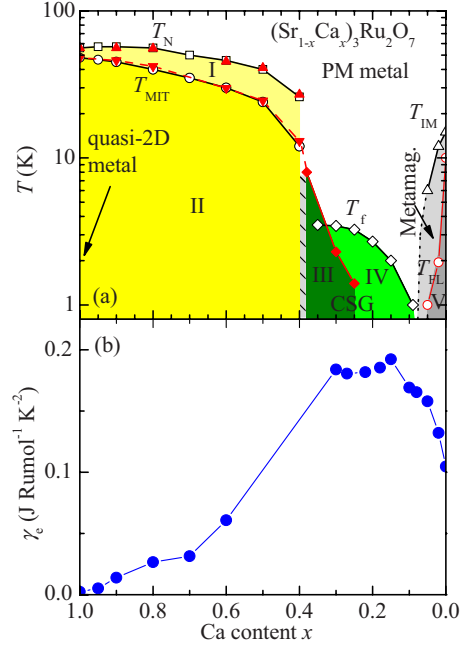

FIG. 8. (Color online) (a) The electronic phase diagram of the double-layered ruthenates $(Sr_{1-x}Ca_x)_3Ru_2O_7$. T_N: Néel temperature; T_{MIT}: metal-insulator transition temperature. The open squares □ and open circles ○ represent T_N and T_{MIT} determined from magnetization measurements,[22] and the filled upward and downward triangles (▲ and ▼) represent those determined from ρ_{ab} measurements. T_f is the freezing temperature for the cluster-spin-glass (CSG) phase.[22] The filled diamond ◆ is the temperature below which the electronic state becomes weakly localized due to magnetic scattering. T_{IM}: the characteristic temperature below which an itinerant metamagnetic phase transition occurs.[22] T_{FL} is the Fermi-liquid temperature. Region I: the AFM metallic state. Region II: the AFM Anderson localized state. Region III: the weakly localized state induced by magnetic scattering. Region IV: the magnetic metallic state (see text). Region V: the metamagnetic Fermi-liquid state. (b) The electronic specific heat coefficient γ_e as a function of Ca content x.

ters an itinerant metamagnetic Fermi-liquid ground state (Region V).

IV. DISCUSSION

First we will discuss the mechanism behind the MIT between Regions I and II. In a strongly correlated electron system, MITs can generally be separated into two categories according to their driving forces,[35] i.e., a Mott transition due to the correlation effect of electrons and an Anderson transition due to disorder. In a typical Mott transition, on-site Coulomb interactions create strongly renormalized quasiparticle states and open a gap at the Fermi level.[36] Therefore, there should be no density of states at Fermi level, resulting in an electronic specific heat equal to zero for a Mott-type insulator. This is well known and has been observed in many materials, e.g., single-layered ruthenate Ca_2RuO_4.[37]

However, the MIT observed in $(Sr_{1-x}Ca_x)_3Ru_2O_7$ for $0.4 \leq x \leq 1.0$ should not be attributed to a typical Mott transition. $Ca_3Ru_2O_7$ was initially thought to be a Mott-like system with

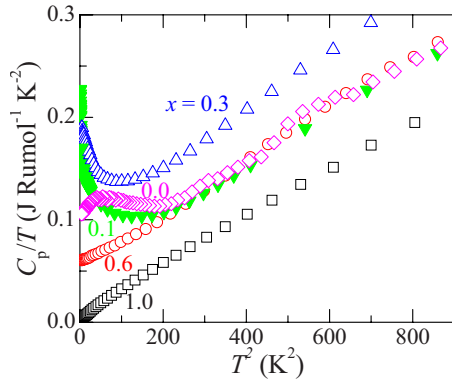FIG. 9. (Color online) Specific heat divided by temperature C/T plotted versus T^2 for typical samples.

FIG. 10. (Color online) Residual in-plane resistivity as a function of the Ca content x. For those samples which show localized behaviors at low temperatures, ρ_{ab} at 0.3 K is taken as the residual in-plane resistivity. The solid curve represents a fit to the Nordheim law $Ax(1-x)$.

a small charge gap ~ 0.1 eV.[16,38,39] But later, an angle-resolved photoemission spectroscopy study revealed that small non-nesting Fermi pockets survive even at lowest achievable temperatures,[24] leading to a small, but nevertheless, nonzero electronic specific heat coefficient (γ_e =1.7 mJ/Ru mol K^2) and a quasi-2D metallic transport behavior.[17] In order to examine how γ_e changes with Sr substitution for Ca, we measured the specific heat of $(Sr_{1-x}Ca_x)_3Ru_2O_7$; the data is shown in Fig. 9. Since the phonon term is proportional to T^3, the phonon contribution can be evaluated by a linear fitting of C/T vs T^2. The electronic specific heat is obtained by subtracting the phonon contribution from the total specific heat. From these analyses, we obtained γ_e for most of our samples, as shown in Fig. 8(b). We find that γ_e is indeed small for $Ca_3Ru_2O_7$, consistent with the previous result;[17] the Sr substitution for Ca gradually increases γ_e, suggesting that the size of FS increases. These results are clearly not expected for a typical Mott insulator, therefore the nonmetallic state observed in Region II cannot be attributed to a Mott insulating state.

Since Sr substitution for Ca introduces disorders to the system, disorder-driven Anderson localization effect should be considered. In general, in the presence of Anderson localization, there exists a finite density of state near the Fermi level, which is localized and does not contribute to conduction.[40] In this scenario, electronic specific heat remains finite despite the system showing nonmetallic behavior. This is precisely in agreement with our observation in Region II. Therefore, the nonmetallic behavior below T_{MIT} should primarily be ascribed to Anderson localization.

As the magnetic state switches from the AFM state to the nearly FM state near $x=0.4$, the electronic state changes to a weakly localized state. Our analyses show that it results from magnetic scattering. As shown in Fig. 3(a), the small upturn of resistivity at low temperature for the $x=0.3$ sample is gradually suppressed by magnetic field and eventually tuned to a quasi-quadratic temperature dependence when the applied field is above 4 T. Similar suppression of the more significant upturn of resistivity in the $x=0.38$ sample is also observed [see the inset to Fig. 3(a)]. These results strongly support the assertion that the weak localization behavior observed for Region III is due to magnetic scattering. In addition, we note that the minimum resistivity occurs close to the
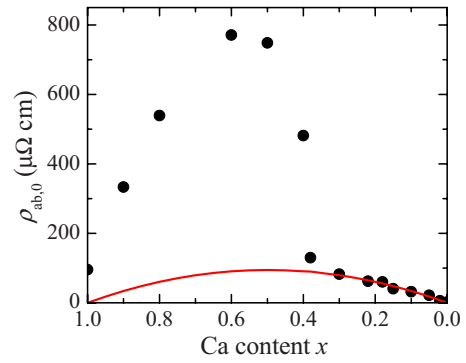
CSG phase freezing temperature T_f. Similar behavior has been observed in many other d- and f-electron spin glasses, such as NiMn,[41] NiMnPt,[42] FeAl$_2$,[43] and U$_2$PdSi$_3$,[44] and it is considered to be associated with the formation of remanent FM domains. For our case, FM correlations are progressively enhanced with lowering temperature, eventually freezing into a CSG phase.[22,23] In the CSG phase the FM clusters are randomly frozen, resulting in strong magnetic scattering among FM clusters. Under the application of magnetic field such magnetic scattering is suppressed, thus suppressing the small upturn of resistivity at low temperatures.

With decreasing Ca content, T_f decreases and FM magnetic correlations become weaker,[22,23] thus reducing magnetic scattering. Consequently, the weakly localized behavior gradually disappears, eventually yielding to a fully metallic state in Region IV. The temperature dependence of resistivity in this metallic state can be fit to $\rho = \rho_0 + AT^\alpha$ at low temperatures with $\alpha > 2$. α is 2.7 for the $x=0.2$ sample; it decreases with a further decrease in x. When $x=0.1$, α is decreased to 2.2, suggesting that the magnetic scattering is still involved in the transport process in this sample. Thus, the electronic state in Region IV can be viewed as a magnetic metallic state. When x is decreased below 0.08, the system enters a metamagnetic state and its electronic state behaves as a Fermi-liquid ground state. As seen in Fig. 7, starting from $x=0$, the Fermi-liquid temperature T_{FL} gradually decreases with increasing x, from 10 K for $x=0$ down to zero for $x \approx 0.08$. We observed a non-Fermi-liquid behavior in the temperature dependence of the electronic specific heat near the critical composition ($x \approx 0.08$) in our early work.[22] Such a non-Fermi-liquid behavior could be attributed to the system approaching a magnetic instability near $x \sim 0.08$.

Although magnetic scattering plays a critical role in transport properties in Regions III and IV, it is still much weaker in comparison with the scattering from the disorder introduced by Ca substation for Sr. This can be clearly seen by fitting residual resistivity to the Nordheim law, which is solely based on disorder-induced scattering. As shown in Fig. 10, the residual in-plane resistivity for $x < 0.4$ can approximately be fitted to the Nordheim formula $Ax(1-x)$ with $A=378$ $\mu\Omega \cdot$cm, implying that the randomness intrinsic to

the Sr/Ca substitution alone can account for the variation in residual resistivity with the Ca content. Only when the electronic state transforms to the Anderson localized state for $x \geq 0.4$, the residual resistivity (taken as the resistivity at 0.3 K) shows a significant deviation from this formula. Another reason for this deviation is that the spin-valve effect sets in for $x \geq 0.4$, which could dramatically affect the residual resistivity.[21]

Comparing the double-layered ruthenates $(Sr_{1-x}Ca_x)_3Ru_2O_7$ to their single-layered analog $Ca_{2-x}Sr_xRuO_4$,[4,5] we note that while they undergo a similar nearly FM-to-AFM transition, distinct differences exist between their electronic states. First, we have shown that the electronic ground state near the Ca side in the double-layered ruthenates is an Anderson localized state, whereas the insulating state near the Ca side in single-layered ruthenates is a Mott insulating state.[4,37] Second, while both solid solutions show CSG phases,[5,22,23] the electronic ground state differs significantly between them: a Fermi-liquid ground state is observed in the CSG phase of $Ca_{2-x}Sr_xRuO_4$,[5] but in the CSG phase of $(Sr_{1-x}Ca_x)_3Ru_2O_7$ the magnetic scattering plays a critical role, resulting in a weakly localized state.

Variations in electronic and magnetic properties in $(Sr_{1-x}Ca_x)_3Ru_2O_7$ can all be attributed to structure changes caused by Ca substitution for Sr. Since Ca^{2+} is smaller than Sr^{2+} in ionic radius, Ca^{2+} substitution for Sr^{2+} should increase structural distortion as in $Ca_{2-x}Sr_xRuO_4$.[45] Consistent with this expectation, Iwata *et al.*[23] observed discontinuous changes in lattice parameters near the boundary between the AFM and the nearly FM phases, and bifurcation of the *a*-axis lattice parameter for $0.6 < x < 1$. From our x-ray diffraction measurements, we observed similar results. Furthermore, we recently performed structure refinement of x-ray diffraction spectra for most of the samples presented in the phase diagram in Fig. 8. We found that the structure distortion caused by the substitution occurs via rotation and tilting of RuO_6 octahedra.[33] Rotation angle gradually increases with Ca substitution for Sr and approaches saturation for $x > 0.6$, whereas the tilting does not occur until the Ca content x is increased above 0.4, and it enhances significantly for $x > 0.6$. These results explain the magnetic phase transitions

observed in this system,[33] the enhanced in-plane magnetic anisotropy for $x > 0.6$,[33] as well as the lattice parameter changes observed by Iwata *et al.*[23] This, together with our observation of complex electronic states described above, suggests strong interplay between charge, spin, and lattice degrees of freedom in double-layered ruthenates.

V. CONCLUSION

In summary, we have established an electronic phase diagram for double-layered ruthenates $(Sr_{1-x}Ca_x)_3Ru_2O_7$. Our results show that the electronic states of this system are complex and strongly coupled with the magnetic states. Disorder has a remarkable effect on electronic transport properties. The electronic ground state in $Ca_3Ru_2O_7$ is quasi-2D metal, but transforms into an Anderson localized state in the AFM region with $0.4 \leq x < 1.0$ due to the presence of disorders introduced by Sr substitution for Ca. When the magnetic state switches from the AFM to the nearly FM state near $x = 0.4$, the electronic state changes to a weakly localized state induced by magnetic scattering for $0.25 \leq x < 0.4$, and then evolves into a magnetic metallic state for $0.08 < x < 0.25$. When x is decreased below 0.08, the system enters a metamagnetic Fermi-liquid ground state. The Fermi-liquid temperature is suppressed to zero near the critical composition with $x \sim 0.08$ and non-Fermi-liquid behavior occurs accordingly. Such complex electronic states coupled with magnetic states testify the strong interplay of charges and spin degrees of freedom in double-layered ruthenates.

*zmao@tulane.edu

[1] A. P. Mackenzie and Y. Maeno, Rev. Mod. Phys. **75**, 657 (2003).

[2] K. Ishida, H. Mukuda, Y. Kitaoka, K. Asayama, Z. Q. Mao, Y. Mori, and Y. Maeno, Nature (London) **396**, 658 (1998).

[3] K. D. Nelson, Z. Q. Mao, Y. Maeno, and Y. Liu, Science **306**, 1151 (2004).

[4] S. Nakatsuji and Y. Maeno, Phys. Rev. Lett. **84**, 2666 (2000).

[5] S. Nakatsuji, D. Hall, L. Balicas, Z. Fisk, K. Sugahara, M. Yoshioka, and Y. Maeno, Phys. Rev. Lett. **90**, 137202 (2003).

[6] R. G. Moore, J. D. Zhang, V. B. Nascimento, R. Jin, J. D. Guo, G. T. Wang, Z. Fang, D. Mandrus, and E. W. Plummer, Science **318**, 615 (2007).

[7] R. A. Borzi, S. A. Grigera, J. Farrell, R. S. Perry, S. J. S. Lister, S. L. Lee, D. A. Tennant, Y. Maeno, and A. P. Mackenzie, Science **315**, 214 (2007).

[8] P. B. Allen, H. Berger, O. Chauvet, L. Forro, T. Jarlborg, A. Junod, B. Revaz, and G. Santi, Phys. Rev. B **53**, 4393 (1996).

[9] G. Cao, S. McCall, M. Shepard, J. E. Crow, and R. P. Guertin, Phys. Rev. B **56**, 321 (1997).

[10] I. Zegkinoglou, J. Strempfer, C. S. Nelson, J. P. Hill, J. Chakhalian, C. Bernhard, J. C. Lang, G. Srajer, H. Fukazawa, S. Nakatsuji, Y. Maeno, and B. Keimer, Phys. Rev. Lett. **95**, 136401 (2005).

[11] M. Kubota, Y. Murakami, M. Mizumaki, H. Ohsumi, N. Ikeda, S. Nakatsuji, H. Fukazawa, and Y. Maeno, Phys. Rev. Lett. **95**, 026401 (2005).

[12] J. F. Karpus, R. Gupta, H. Barath, S. L. Cooper, and G. Cao, Phys. Rev. Lett. **93**, 167205 (2004).

[13] S.-I. Ikeda, Y. Maeno, S. Nakatsuji, M. Kosaka, and Y. Uwatoko, Phys. Rev. B **62**, R6089 (2000).

[14] R. S. Perry, L. M. Galvin, S. A. Grigera, L. Capogna, A. J. Schofield, A. P. Mackenzie, M. Chiao, S. R. Julian, S. I. Ikeda, S. Nakatsuji, Y. Maeno, and C. Pfleiderer, Phys. Rev. Lett. **86**, 2661 (2001).

[15] S. A. Grigera, R. S. Perry, A. J. Schofield, M. Chiao, S. R. Julian, G. G. Lonzarich, S. I. Ikeda, Y. Maeno, A. J. Millis, and A. P. Mackenzie, Science **294**, 329 (2001).

[16] G. Cao, S. McCall, J. E. Crow, and R. P. Guertin, Phys. Rev. Lett. **78**, 1751 (1997).

[17] Y. Yoshida, I. Nagai, S.-I. Ikeda, N. Shirakawa, M. Kosaka, and N. Môri, Phys. Rev. B **69**, 220411(R) (2004).

[18] G. Cao, L. Balicas, Y. Xin, E. Dagotto, J. E. Crow, C. S. Nelson, and D. F. Agterberg, Phys. Rev. B **67**, 060406(R) (2003).

[19] D. J. Singh and S. Auluck, Phys. Rev. Lett. **96**, 097203 (2006).

[20] Y. Yoshida, S.-I. Ikeda, H. Matsuhata, N. Shirakawa, C. H. Lee, and S. Katano, Phys. Rev. B **72**, 054412 (2005).

[21] W. Bao, Z. Q. Mao, Z. Qu, and J. W. Lynn, Phys. Rev. Lett. **100**, 247203 (2008).

[22] Z. Qu, L. Spinu, H. Q. Yuan, V. Dobrosavljevic, W. Bao, J. W. Lynn, M. Nicklas, J. Peng, T. J. Liu, D. Fobes, E. Flesch, and Z. Q. Mao, Phys. Rev. B **78**, 180407(R) (2008).

[23] K. Iwata, Y. Yoshida, M. Kosaka, and S. Katano, J. Phys. Soc. Jpn. **77**, 104716 (2008).

[24] F. Baumberger, N. J. C. Ingle, N. Kikugawa, M. A. Hossain, W. Meevasana, R. S. Perry, K. M. Shen, D. H. Lu, A. Damascelli, A. Rost, A. P. Mackenzie, Z. Hussain, and Z.-X. Shen, Phys. Rev. Lett. **96**, 107601 (2006).

[25] J. S. Lee, S. J. Moon, B. J. Yang, J. Yu, U. Schade, Y. Yoshida, S.-I. Ikeda, and T. W. Noh, Phys. Rev. Lett. **98**, 097403 (2007).

[26] S. Chikara, V. Durairaj, W. H. Song, Y. P. Sun, X. N. Lin, A. Douglass, G. Cao, P. Schlottmann, and S. Parkin, Phys. Rev. B **73**, 224420 (2006).

[27] T. Oguchi, Phys. Rev. B **51**, 1385 (1995).

[28] D. J. Singh, Phys. Rev. B **52**, 1358 (1995).

[29] A. P. Mackenzie, S. R. Julian, A. J. Diver, G. J. McMullan, M. P. Ray, G. G. Lonzarich, Y. Maeno, S. Nishizaki, and T. Fujita, Phys. Rev. Lett. **76**, 3786 (1996).

[30] A. Damascelli, D. H. Lu, K. M. Shen, N. P. Armitage, F. Ronning, D. L. Feng, C. Kim, Z.-X. Shen, T. Kimura, Y. Tokura, Z. Q. Mao, and Y. Maeno, Phys. Rev. Lett. **85**, 5194 (2000).

[31] K. M. Shen, A. Damascelli, D. H. Lu, N. P. Armitage, F. Ronning, D. L. Feng, C. Kim, Z.-X. Shen, D. J. Singh, I. I. Mazin, S. Nakatsuji, Z. Q. Mao, Y. Maeno, T. Kimura, and Y. Tokura, Phys. Rev. B **64**, 180502(R) (2001).

[32] D. Forsythe, S. R. Julian, C. Bergemann, E. Pugh, M. J. Steiner, P. L. Alireza, G. J. McMullan, F. Nakamura, R. K. W. Haselwimmer, I. R. Walker, S. S. Saxena, G. G. Lonzarich, A. P. Mackenzie, Z. Q. Mao, and Y. Maeno, Phys. Rev. Lett. **89**, 166402 (2002).

[33] J. Peng, Z. Qu, B. Qian, D. Fobes, T. J. Liu, X. S. Wu, H. M. Pham, L. Spinu, and Z. Q. Mao (unpublished).

[34] S. McCall, G. Cao, and J. E. Crow, Phys. Rev. B **67**, 094427 (2003).

[35] M. Imada, A. Fujimori, and Y. Tokura, Rev. Mod. Phys. **70**, 1039 (1998).

[36] A. Georges, G. Kotliar, W. Krauth, and M. J. Rozenberg, Rev. Mod. Phys. **68**, 13 (1996).

[37] H. Fukazawa and Y. Maeno, J. Phys. Soc. Jpn. **70**, 460 (2001).

[38] G. Cao, K. Abbound, S. McCall, J. E. Crow, and R. P. Guertin, Phys. Rev. B **62**, 998 (2000).

[39] H. L. Liu, S. Yoon, S. L. Cooper, G. Cao, and J. E. Crow, Phys. Rev. B **60**, R6980 (1999).

[40] P. A. Lee and T. V. Ramakrishnan, Rev. Mod. Phys. **57**, 287 (1985).

[41] S. Senoussi and Y. Öner, Phys. Rev. B **28**, 455 (1983).

[42] H. Z. Durusoy and Y. Öner, Phys. Rev. B **42**, 6831 (1990).

[43] C. S. Lue, Y. Öner, D. G. Naugle, and J. H. Ross, Jr., Phys. Rev. B **63**, 184405 (2001).

[44] D. X. Li, Y. Shiokawa, Y. Homma, A. Uesawa, A. Dönni, T. Suzuki, Y. Haga, E. Yamamoto, T. Honma, and Y. Ōnuki, Phys. Rev. B **57**, 7434 (1998).

[45] O. Friedt, M. Braden, G. André, P. Adelmann, S. Nakatsuji, and Y. Maeno, Phys. Rev. B **63**, 174432 (2001).